An investigation into the curing of urushi and tung oil films by thermoanalytical and mass spectrometric techniques

Diego Tamburini[1, †], *Dario Sardi*[1], *Alessio Spepi*[1], *Celia Duce*[1], *Maria Rosaria Tinè*[1], *Maria Perla Colombini*[1,2], *Ilaria Bonaduce*[1]*.

[1] Department of Chemistry and Industrial Chemistry, University of Pisa, via Giuseppe Moruzzi 13, I-56124, Pisa, Italy

[2] Institute for the Conservation and Valorization of Cultural Heritage (ICVBC), National Research Council, via Madonna del Piano 10, Sesto Fiorentino, I-50019 Florence, Italy.

KEYWORDS: urushi, tung oil, curing, mass spectrometry, Py-GC-MS, EG-MS, EGA-MS, TG, DSC, autoxidation.

ABSTRACT. Urushi is the oldest and most precious lacquer used since antiquity in East Asia. For artistic purposes, in order to obtain suitable rheological properties, the lacquer is usually mixed with a vegetable oil. In this work we investigated the curing process of urushi/tung oil mixtures in order to highlight the chemical interactions at the molecular level between the two materials.

A multi-analytical approach was adopted, based on thermogravimetry (TG), differential scanning calorimetry (DSC), gas chromatography-mass spectrometry (GC-MS), evolved gas analysis-mass spectrometry (EGA-MS), analytical pyrolysis coupled with gas chromatography and mass spectrometry (Py-GC-MS) and high performance liquid chromatography-mass spectrometry (HPLC-MS). Fresh and aged mixtures were analysed and the results were compared with those obtained from the analysis of the individual materials.

The data highlighted that different polymerization and oxidation mechanisms take place in oil/urushi mixtures compared to the pure materials. Py-GC-MS and GC-MS showed that the profile of aliphatic mono- and di-carboxylic acids was drastically different for the aged film of pure tung oil compared to the mixtures. The ratio between the relative content of azelaic and palmitic acids was much lower in the mixtures than in the pure oil, highlighting a lower level of oxidation. On the other hand, the relative content of short chain carboxylic acids, which are produced by pyrolysis of the cross-linked oil network, increased as the concentration of urushi in the mixtures increased, thus indicating an increasing level of reticulation. HPLC-MS showed a relatively higher amount of triglycerides with hydroxylated fatty acids – the intermediate oxidation product of polyunsaturated fatty acids - in the mixtures with respect to pure tung oil.

1. INTRODUCTION

Tung oil and urushi are two natural organic materials, which spontaneously form solid long-lasting films. This feature makes these materials extremely suitable for artistic and protective purposes. Tung oil has long been used as a binding medium [1-3] and as a coating material, especially for wooden artefacts [4]. Urushi lacquer is considered as the oldest and most precious lacquer in East Asia, and has been used for thousands of years as a coating material, because of its capacity to lend great and lasting brightness, toughness and water resistance to the object [5].

Tung oil is a vegetable oil extracted from the nuts of the tung tree (*Vernicia fordii*). Its triglyceride composition mainly consists of polyunsaturated fatty acids. In particular, α-eleostearic acid ((9*Z*,11*E*,13*E*)-octadeca-9,11,13-trienoic acid) accounts for *ca.* 80 % of the fatty acids [6]. Tung oil thus belongs to the group of drying oils that polymerise under exposure to air and light [7].

This process is referred to as autoxidation, a well-studied free-radical chain reaction, which can be divided into three main steps: 1) beginning, 2) propagation , 3) termination [8].

In the first step a radical initiator begins the formation of radicals by H-abstraction from the unsaturated alkyl chains of fatty acids. Allylic and in particular bis-allylic positions are favoured for this process, because the radicals formed are stabilised by resonance. The second step involves the attack of molecular oxygen to form peroxyl radicals. The peroxyl radicals can perform an H-abstraction from another chain, propagating the reaction and forming hydroperoxides, which are considered as the first oxidation products of polyunsaturated fatty acids [9]. Hydroperoxides can further degrade to form alkoxyl and hydroxyl radicals, which contribute to propagate the reaction. During these two phases, for unconjugated fatty acids, H-abstraction to form radicals is highly preferred with respect to the addition of a radical to double

bonds, which is instead favoured in conjugated fatty acids, especially when they are in cis-configuration [10]. The formation of a cross-linked network, as well as of cyclic peroxides or polyperoxides is a consequence of this latter phenomenon [10-13].

The termination step includes all the cross-linking reactions where two radicals are combined to form non-radical, stable species, leading to the formation of C-C and C-O-C bonds. For conjugated systems, the disproportion of the compounds formed by the addition of a radical to a double bond can also occur [14]. The decomposition of primarily formed hydroperoxides and peroxides can also be followed by β-scission and other side reactions, leading to the formation of low molecular weight compounds, such as alcohols, ketones, aldehydes, acids, and alkanes [8,15-18]. The photo- and thermo- instability of alcohols, aldehydes and ketones, and the presence of oxygen create favourable conditions for the production of dicarboxylic acids, which are considered as the final oxidation products in these systems [15,19].

Urushi is a lacquer produced from the sap of the *Rhus Vernicifera* tree. The sap is composed of water (30%), glycoproteins (2%), plant gum (7%), laccase enzyme (1%), and a mixture of catechol derivatives (60-65%) referred to as urushiol [20]. The most abundant catechol in urushiol is (8*Z*,11*E*,13*Z*)-3-pentadecatrienylcatechol [21]. Laccase enzyme is a copper-containing enzyme, fundamental in the polymerisation of urushi, as it catalyses the reduction of Cu^{2+} to Cu^{+}, which reacts with oxygen to form a peroxyl intermediate. The peroxyl intermediate reacts with the catechol, leading to the formation of a semiquinone radical and to the loss of a water molecule. The semiquinone radicals react with each other to form C-C bonds between two aromatic nuclei (biphenyl dimers, trimers, etc.). With further electron transfer, quinone species are formed, which can react with the unsaturated side chains to form C-C bonds between aromatic nuclei and aliphatic chains, and C-O bonds between phenolic oxygens and aliphatic chains[22]. These

mechanisms consume the urushiol monomers, and when their concentration drops below 30%, auto-oxidation reactions take place at the side chains, according to the same mechanisms described for polyunsaturated fatty acids [20,23,24].

Tung oil and urushi have often been used in mixtures in oriental art [25], as the resulting film shows enhanced rheological and mechanical properties. The mixture dries more slowly and the resulting film is less hard than that obtained with pure lacquer, thus facilitating manual polishing to obtain the finishing layers.

Despite much research has been dedicated in the literature at improving the quality of urushi lacquer films, acting on its formulation or on its curing[23,26-28], molecular studies of the curing and quality of the film that is produced by mixing urushi and tung oil have not been reported.

The aim of this study was to understand the chemical interactions taking place at the molecular level between the two materials when they cure together. We also investigated whether it is possible to identify one or more molecular markers that can be used to determine whether tung oil and urushi belong to the same layer, and thus curing occurred at the same time, or if they were applied in two distinct layers, and thus curing occurred separately.

We used a multi-analytical approach, based on thermogravimetry (TG), differential scanning calorimetry (DSC), gas chromatography-mass spectrometry (GC-MS), evolved gas analysis-mass spectrometry (EGA-MS), analytical pyrolysis coupled with gas chromatography and mass spectrometry (Py-GC-MS) and high performance liquid chromatography-mass spectrometry (HPLC-MS). The study revealed that urushi acts as an antioxidant, favouring the cross-linking of the oil polyunsaturated fatty acids over oxidation. Copolymerisation between the two materials also takes place and auto-oxidation reactions of catechol alkyl substituents occur at a higher rate in urushi, when it is mixed with tung oil.

2. EXPERIMENTAL SECTION

2.1 Reagents. Lauric acid, suberic acid, myristic acid, azelaic acid, sebacic acid, palmitic acid, oleic acid, stearic acid, tridecanoic acid, hexadecane (Sigma-Aldrich, 99% purity). Acetone, diethyl ether, ethanol, n-hexane and isooctane (Sigma-Aldrich, HPLC grade). *N,O*-bis(trimethylsilyl)-trifluoroacetamide (BSTFA) with 1% trimethylchlorosilane (TMCS) (Sigma-Aldrich, 98.5% purity). 1,1,1,3,3,3-hexamethyldisilazane (HMDS) (Sigma-Aldrich, purity 99,9%). The solvents used for the HPLC analyses were: *iso*-propanol, *n*-hexane, trichloromethane and methanol (HPLC/MS grade; Fluka, U.S.).

2.2. Samples. Tung oil was purchased by Kremer Pigmente and the raw material for urushi lacquer was bought from a local producer in the northern slopes of the Qinling mountains near Xi'an (China) in 2007. Both fresh and aged samples were analysed. Fresh tung oil, fresh urushi and a 1:1 (w/w) fresh mixture of the two materials (M1*) were used for TG and DSC analyses. Films were prepared by depositing a few milligrams of the materials on laboratory glass plates. The tung oil film was analysed after two years of natural ageing. Films of urushi and mixtures of urushi and tung oil in w/w ratios 1:1 (M1), 2:1 (M2) and 4:1 (M4) were prepared in 2007 and analysed after eight years of natural ageing. These samples were analysed by mass spectrometric techniques.

2.3. TG and DSC. A TA Instruments Thermobalance model Q5000IR was used. Isothermal experiments were performed on fresh materials under a constant air flow (90 mL min^{-1}) at 80°C

for 6000 min (*ca*. four days). The amount of sample used for these analyses ranged from 3 to 4 mg. DSC measurements were performed by a Perkin Elmer Pyris Diamond Differential Scanning Calorimeter in the temperature range of 30-300 °C, with a heating rate of 10 °C min^{-1} and using nitrogen as purging gas. Fresh tung oil and a 1:1 (w/w) fresh mixture of the two materials (M1*) were analysed after different curing times: 0, 3, 21, 45, 93, 140, 190, 282, 450 and 2800 hours. The amount of sample used for these analyses ranged from 5 to 6 mg, and samples were prepared in aluminium pans.

2.4. EGA-MS. The instrumentation consisted of a micro-furnace Multi-Shot Pyrolyzer EGA/Py-3030D (Frontier Lab) coupled with a gas chromatograph 6890 Agilent Technologies (Palo Alto, USA) equipped with a deactivated and uncoated stainless steel transfer tube (UADTM-2.5N, 0.15mm i.d.×2.5m length, Frontier Lab). The GC was coupled with a 5973 Agilent Mass Selective Detector (Palo Alto, USA) single quadrupole mass spectrometer. The temperature of the micro-furnace chamber was programmed from 50°C to 800°C, with a rate 10°C min^{-1}. Analyses were performed under a helium flow (1mL min^{-1}) and samples were introduced with a split ratio 1:20. The micro-furnace interface temperature was kept at 100°C higher than the furnace temperature until the maximum value of 300°C. The inlet temperature was 280°C. The chromatographic oven was kept at 300°C. The mass spectrometer was operated in EI positive mode (70 eV, scanning *m/z* 50-600). The MS transfer line temperature was 300°C. The MS ion source temperature was kept at 230°C, and the MS quadrupole temperature at 150°C. A total of 0.5 mg of sample was put into a stainless steel cup and inserted into the micro-furnace. The sample underwent a thermal decomposition in inert atmosphere over the chosen

heating range. The evolved gaseous compounds were directly transferred to the mass spectrometer, where they were ionised and analysed as a function of time.

2.5. GC-MS. Standard solutions of lauric acid (5,216 μg/g), suberic acid (5,474 μg/g), myristic acid (3,889 μg/g), azelaic acid (3,844 μg/g), sebacic acid (4,128 μg/g), palmitic acid (4,530 μg/g), oleic acid (6,279 μg/g), and stearic acid (6,198 μg/g) were made in acetone. Different volumes of the standard solutions were used to obtain calibration curves, with which the concentration of the fatty acids in the samples was then calculated. Tridecanoic acid and hexadecane were used as internal standards for derivatisation and injection, respectively.

A weighted amount of sample (*ca.* 0.5 mg) was added to 300 μL of ethanolic KOH (10% w/w) and underwent microwave-assisted saponification. A microwave oven model ETHOS One (Milestone, Sorisole, Bergamo, Italy), operating at 80°C, 200W for 60 minutes was used for the saponification. The alcoholic solution was acidified with HCl 6M, and underwent extraction with hexane (200 μL×3) and diethyl ether (200 μL × 3). 50 μL of the extract was added with 5 μL of tridecanoic acid and dried under N_2. 20 μL of BSTFA with 1% of TMCS and the solution was put in a water bath at 60 °C for 5 min. 50 μL of isooctane were then added and the solution was put again in the water bath for 25 min. 100 μL of isooctane and 10 μL of hexadecane were then added and 2 μL of the solution were finally analysed by GC/MS. Analyses were performed in triplicate.

A gas chromatograph 6890N GC System (Agilent Technologies, Palo Alto, CA, USA) coupled with a 5975 Mass Selective Detector (Agilent Technologies, Palo Alto, CA, USA) single quadrupole mass spectrometer was used. For the gas chromatographic separation, an HP-5ms fused silica capillary column (5%-diphenyl / 95%-dimethyl polysiloxane, 30m × 0.25mm i.d.,

0.25 μm film thickness (J&W Scientific, Agilent Technologies, Palo Alto, CA) with a deactivated silica pre-column (2 m × 0.32 mm i.d., (J&WScientific Agilent Technologies, Palo Alto, CA) was used. The PTV injector was used in splitless mode at 280 °C. The carrier gas was used in the constant flow mode (He, purity 99.995%) at 1.0 mL min^{-1}. The chromatographic oven was programmed as follows: initial temperature 80 °C, isothermal for 2 min; 10 °C min^{-1} up to 200 °C, and isothermal for 3 min; 10 °C min^{-1} up to 280 °C, and isothermal for 30 min. The MS transfer line temperature was 280 °C; the MS ion source temperature was 230 °C, and the MS quadrupole temperature was 150 °C. The mass spectrometer operated in EI positive mode (70 eV) with a scan range *m/z* 50-700. MS spectra were recorded both in TIC (total ion current) and SIM (single ion monitoring) mode.

2.6. Py (HMDS)-GC-MS. 1,1,1,3,3,3-hexamethyldisilazane (HMDS) was used as a silylating agent for the *in situ* derivatisation of pyrolysis products. The instrumentation consisted of a micro-furnace Multi-Shot Pyrolyzer EGA/Py-3030D (Frontier Lab) coupled to a gas chromatograph 6890 (Agilent Technologies, Palo Alto, CA, USA) and to an Agilent 5973 Mass Selective Detector operating in electron impact mode (EI) at 70 eV. The only difference with the gas chromatograph used for GC/MS analysis was the injector, which was a split/splitless injector used with at 1:20 split ratio and kept at 280 °C. The pyrolysis temperature was 550 °C and interface temperature was 280 °C. *Ca*. 100 μg of sample were admixed with 3 μL HMDS into a stainless steel cup and inserted into the micro-furnace. Chromatographic conditions were as follows: initial temperature 36 °C, 10 min isothermal; 10 °C min^{-1} up to 280 °C, 2 min isothermal; 20°C min^{-1} up to 310 °C, 50 min isothermal. Carrier gas: He (purity 99.995%), constant flow 1.0 mL min^{-1}. Analyses were performed in triplicate.

2.7. HPLC-ESI-Q-ToF. HPLC-ESI-Q-ToF analyses were carried out using a 1200 Infinity HPLC, coupled with a Quadrupole-Time of Flight tandem mass spectrometer 6530 Infinity Q-ToF detector by a Jet Stream ESI interface (Agilent Technologies). The HPLC conditions were: Poroshell 120 EC-C18 column (3.0 mm × 5.0 mm, 2.7 μm particle size) with a Zorbax eclipse plus C-18 guard column (4.6 mm × 12.5 mm, 5 μm particle size); a flow rate of 0.3 mL/min, an injection volume of 1 μL and a column temperature of 45 °C. Separation was achieved using a gradient of methanol (eluent A) and iso-propanol (eluent B). The elution gradient was programmed as follows: 90% A for 5 min, followed by a linear gradient to 90% B in 25 min, then held for 5 min. Re-equilibration time for each analysis was 10 min. The ESI operating conditions were: drying gas (N_2, purity >98%): 350 °C and 10 L/min; capillary voltage 4.5 KV; nebulizer gas 35 psig; sheath gas (N_2, purity >98%): 375 °C and 11 L/min. High resolution MS and MS/MS spectra were acquired in positive mode in the range 100 e1700 *m/z*. The fragmentor was kept at 200 V, nozzle voltage

1000 V, skimmer 65 V, octapole RF 750 V. For the MS/MS experiments, voltages in the range 30-100 V in the collision cell were tested for Collision Induced Dissociation (CID), to obtain information on fragmentation pathways of selected analytes. The MS/MS spectra were obtained at 50 V. The collision gas was nitrogen (purity 99.999%). The data were collected by auto MS/MS acquisition with an MS scan rate of 1.03 spectra/sec and an MS/MS scan rate of 1.05 spectra/sec; only one precursor was acquired per cycle (relative threshold 0.010%). The mass axis was calibrated daily using the Agilent tuning mix HP0321 (Agilent Technologies).

MassHunter® Workstation Software (B.04.00) was used to carry out mass spectrometer control, data acquisition, and data analysis.

For the HPLC/MS analyses, 0.1-0.8 mg of each paint sample were subjected to extraction assisted by Milestone microwaves Ethos One (power 600 W) with 300 μL of a trichloromethane:hexane (3:2) mixture at 80 °C for 25 min. The extracts were dried under a nitrogen stream, diluted with 600 μL of elution mixture and filtered on a 0.45 mm PTFE filter (Grace Davison Discovery Sciences, U.S.) just before injection [29].

3. RESULTS AND DISCUSSION

3.1. TG and DSC. In order to monitor the curing of the different materials and their mixtures, the oxygen uptake curve was registered, which monitors the weight changes of the sample under a flow of air at a constant temperature (80°C). Figure 1 reports the oxygen uptake curves of fresh tung oil, urushi and the fresh 1:1 mixture M1*.

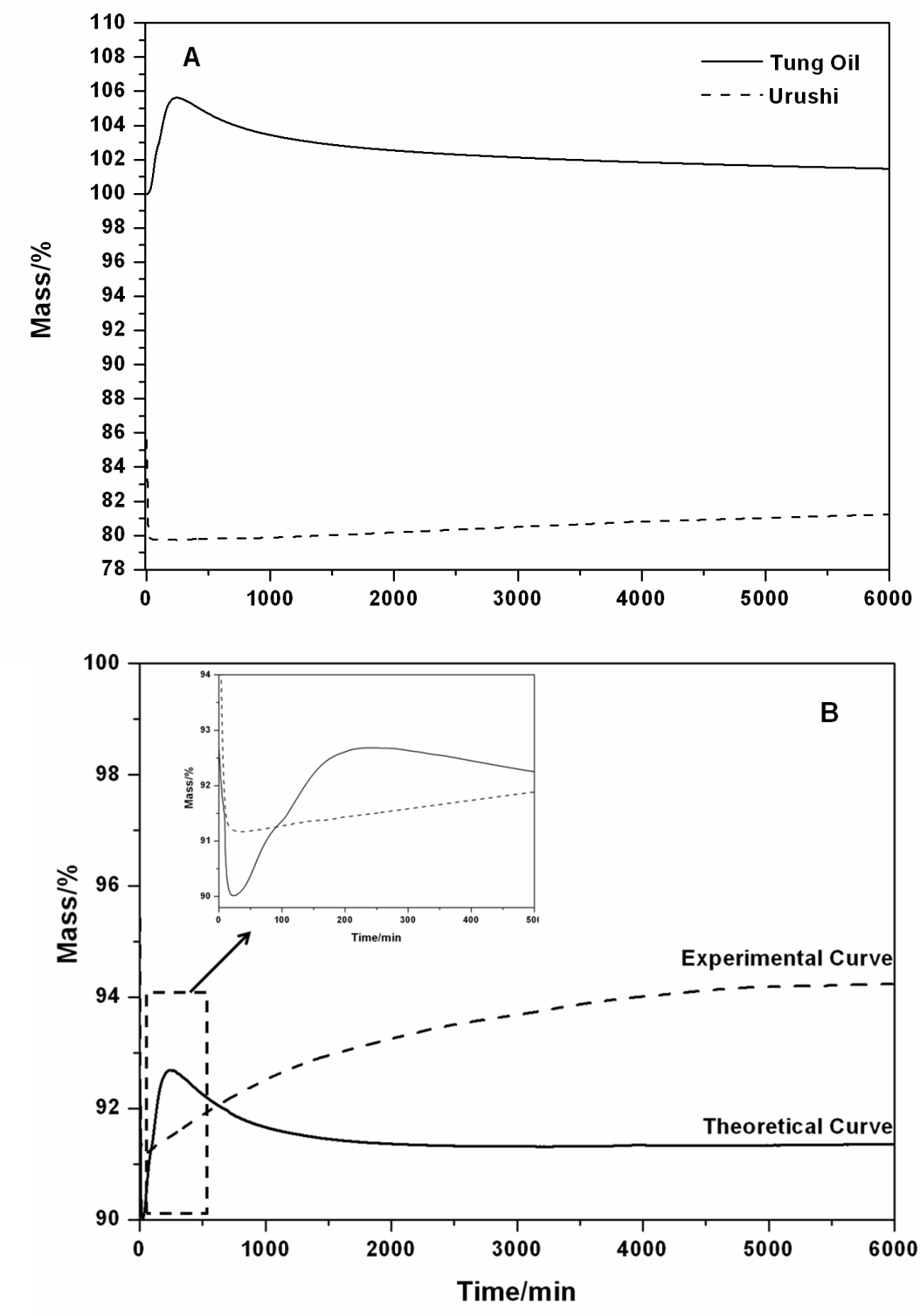

Figure 1. Percentage mass changes of **A)** fresh tung oil and urushi and B) M1* (theoretical and experimental) treated under air flow at a constant temperature of 80°C versus time of treatment.

Tung oil showed a rapid oxygen uptake in the first three hours up to 4.1 % due to the formation of peroxides and hydroperoxides. After this period a mass loss was observed, due to the decomposition of these compounds and the evaporation of volatile molecules formed as a consequence of β-scission reactions [16-18,30,31]. After four days the mass increase was 1 % and appeared to reach a plateau. This is due to the oxygen that remains in the oil film in the form of acidic moieties in dicarboxylic acids, and the oxygen that is incorporated into the polymeric network in the form of ether moieties.

Urushi showed an initial mass loss of around 20 %, as a consequence of water evaporation. A very slow increase in mass up to 1.5 % was observed, which can be ascribed to autoxidation reactions involving the unsaturated side chains of urushi monomers [20,24].

The mixture of urushi and tung oil showed the initial weight loss ascribable to water evaporation, which accounted for 10 % of the initial mass, in agreement with the composition of the mixture. After this, a slow mass increase up to 3 % was recorded after four days of experiments. By comparing the experimental curve with the theoretical curve, calculated on the basis of the curves of the pure materials (Figure 1 B), we can conclude that the curing of the mixture follows different pathways than those undergone by the pure materials alone. In addition, clearly more oxygen remains incorporated into the network in the form of stable, non-volatile compounds.

DSC analyses confirmed that the kinetics and the mechanisms of the autoxidation of unsaturated alkyl chains of tung oil were drastically modified by the addition of urushi. Figure 2 shows the DSC curves of freshly-prepared films of tung oil (a) and M1* (b), recorded immediately after application, and subsequently after different curing times up to 2800h.

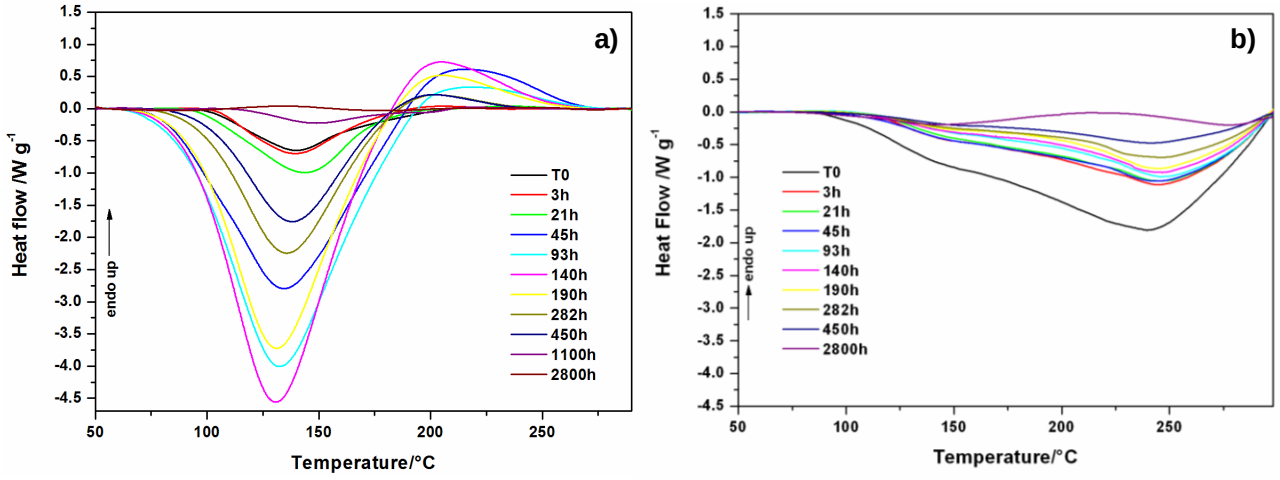

Figure 2. DSC curves of freshly prepared films of a) tung oil and b) M1*, recorded immediately after application, and subsequently at different curing times up to 2800h. Measurements were undertaken under nitrogen flow in the temperature range 50-300°C.

The DSC signal observed in the temperature range 50-300°C can be ascribed to free-radical chain reactions, referred to as propagation (oxygen uptake) and termination. The endothermic homolytic scission of the O-O bond and the subsequent exothermic recombination of the radicals formed generally results in a globally exothermic process. The shape of the DSC exothermic peak can appear as a single broad band or as a more structured band where two (partially resolved) peaks are visible during ageing [32-34]. According to the literature, the peak at lower temperatures, about 150°C, is mostly due to autoxidation, whereas the thermal effect at about 250°C can be ascribed to propagation and cross-linking reactions [32,34-37].

The autoxidation of tung oil had the typical behaviour of a drying oil with a single broad exothermic band [35,36] at about 130°C, which indicates that there is a prevalence of autoxidation reactions. The exothermic signal showed its maximum value after 140 h of curing, indicating that

the network contained the highest concentration of peroxide moieties after around six days. The signal slowly decreased to almost zero after 2800 h, indicating that curing can be considered complete after around three months. The small endothermic residual peak visible at the end of each exothermic peak could be partially due to the evaporation of volatile oxygenated by-products, formed as a result of β-scission reactions in the autoxidation of polyunsaturated fatty acids, in agreement with the isothermal TG experiments (see Fig. 1).

For the mixture M1*, DSC profiles drastically changed. Two exothermic effects at about 140 and 240°C were clearly present, showing a maximum intensity for the fresh mixture (T_0). The thermal effects ascribable to autoxidation phenomena (T_{max}= 140°C) and to propagation and cross linking reactions (T_{max}= 240°C), were there well separated. The relative intensities of the peaks also indicate that in the case of the tung oil mixture, triglycerides undergo a higher rate of propagation and cross-linking and a lower rate of oxidation when tung oil cures in the presence of urushi.

3.2. EGA-MS. Evolved gas analysis mass spectrometry provides information on the thermochemistry of materials. This information can then be integrated with the highly detailed molecular data obtained by mass spectrometry. In this work EGA-MS was used to investigate the behaviour of the cured materials towards thermal degradation. Figure 3 shows the total ion thermograms of the aged films of tung oil, urushi and M1.

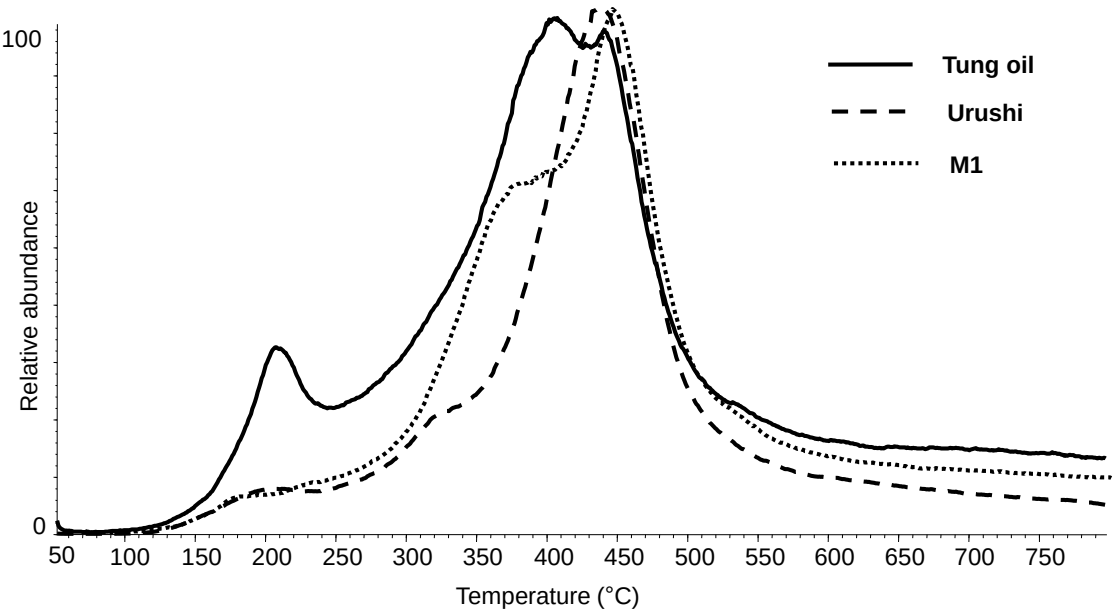

Figure 3. Total ion thermograms obtained by EGA-MS analysis of the aged films of tung oil, urushi and M1.

Thermal degradation occurred in similar temperature ranges for the pure materials and the mixture (100-550°C). Three main thermal degradation regions were highlighted for tung oil. The first region showed a maximum around 210°C. The mass spectra in this region (Figure 4) showed the typical features of fatty acid fragmentation under EI. In particular, the mass spectra showed signals at *m/z* 152, 256 and 284, corresponding to the $[M\text{-}2H_2O]^{\cdot+}$ fragment ion for azelaic acid, and the molecular ions for palmitic and stearic acids, respectively. Therefore, the peak observed in this region is due to the thermal desorption of free fatty acids originating from hydrolysis of the oil under ageing. The second region showed a maximum around 400°C and the mass spectra in this region highlighted a relative abundance of signals at *m/z* 171, 185, 199 and 213 (Figure 4) ascribable to fragment ions with formula $[M\text{-}CH_3(CH_2)_n]^{\cdot+}$ due to the EI mass fragmentation of glycerides. The third region with a maximum around 430°C revealed the

fragmentation of the polymeric network. In fact, fragment ions with *m/z* 91 and 105, ascribed to aromatic structures, dominated the mass spectra (Figure 4). These species are produced in the pyrolysis of the cross-linked aliphatic chains.

As far as urushi is concerned, the first shoulder between 100 and 200°C could be ascribed to the volatilisation of glycerol, added as an additive to the commercial lacquer [30]. Another shoulder around 320°C was detected and then a main decomposition region with a maximum around 440°C was present in the thermogram. The mass spectra from the shoulder and the main region showed very similar profiles, thus indicating that they were formed by materials with a very similar molecular composition but different degree of polymerisation. The mass spectra showed the presence of fragment ions typical of aliphatic chains (*m/z* 55, 69), aromatic structures (*m/z* 91), phenols (*m/z* 108), and catechols (*m/z* 123). The fragment ions at *m/z* 208 e 320, corresponding to the molecular ions of heptylcatechols and pentadecylcatechols respectively, were also detected (Figure 4).

The thermogram obtained for the mixture M1 showed the features of a combination of the thermograms of the two pure materials. The other mixtures M2 and M4 gave similar results to M1, although showing a reduction in the signals ascribable to the degradation of the less abundant triglycerides.

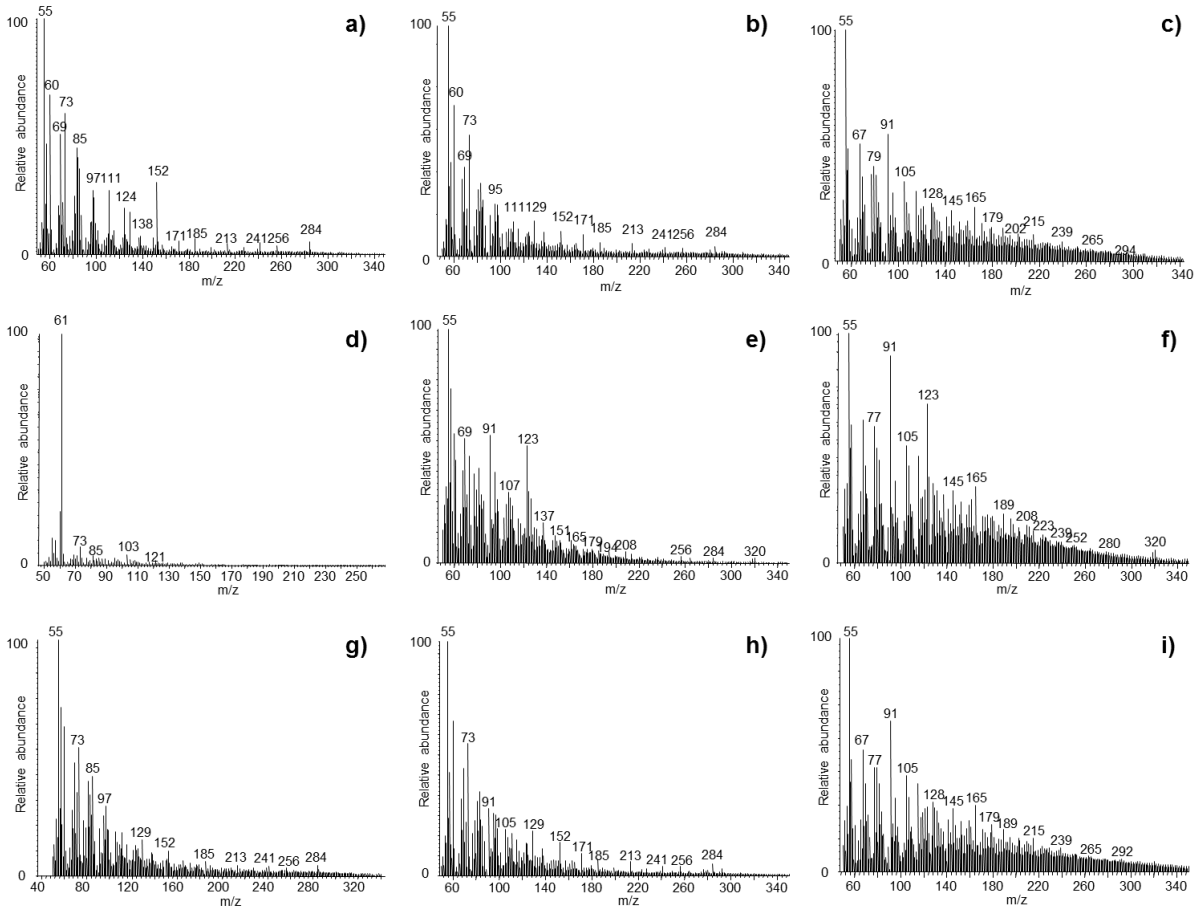

Figure 4. Average mass spectra obtained by EGA-MS of tung oil (a, b and c), urushi (d, e and f) and mixture M1 (g, h and i). The average mass spectra correspond to the main thermal degradation regions. For tung oil: a) 10-20 min (150-250°C); b) 20-37 min (250-420°C); c) 38-45 min (430-500°C). For urushi: d) 8-20 min (130-250°C); e) 20-30 min (250-350°C); f) 30-48 (350-530°C). For mixture M1: g) 10-20 min (150-250°C); h) 20-35 min (250-400°C); i) 35-48 (400-530°C).

EGA-MS analysis enables specific fragment ions to be extracted in order to follow their evolution during the scanned temperature range. We thus selected the fragment ions with *m/z* 91,

108, 123, 152, 256 and 284, and Figure 5 reports the extract ion thermograms for tung oil, urushi and M1.

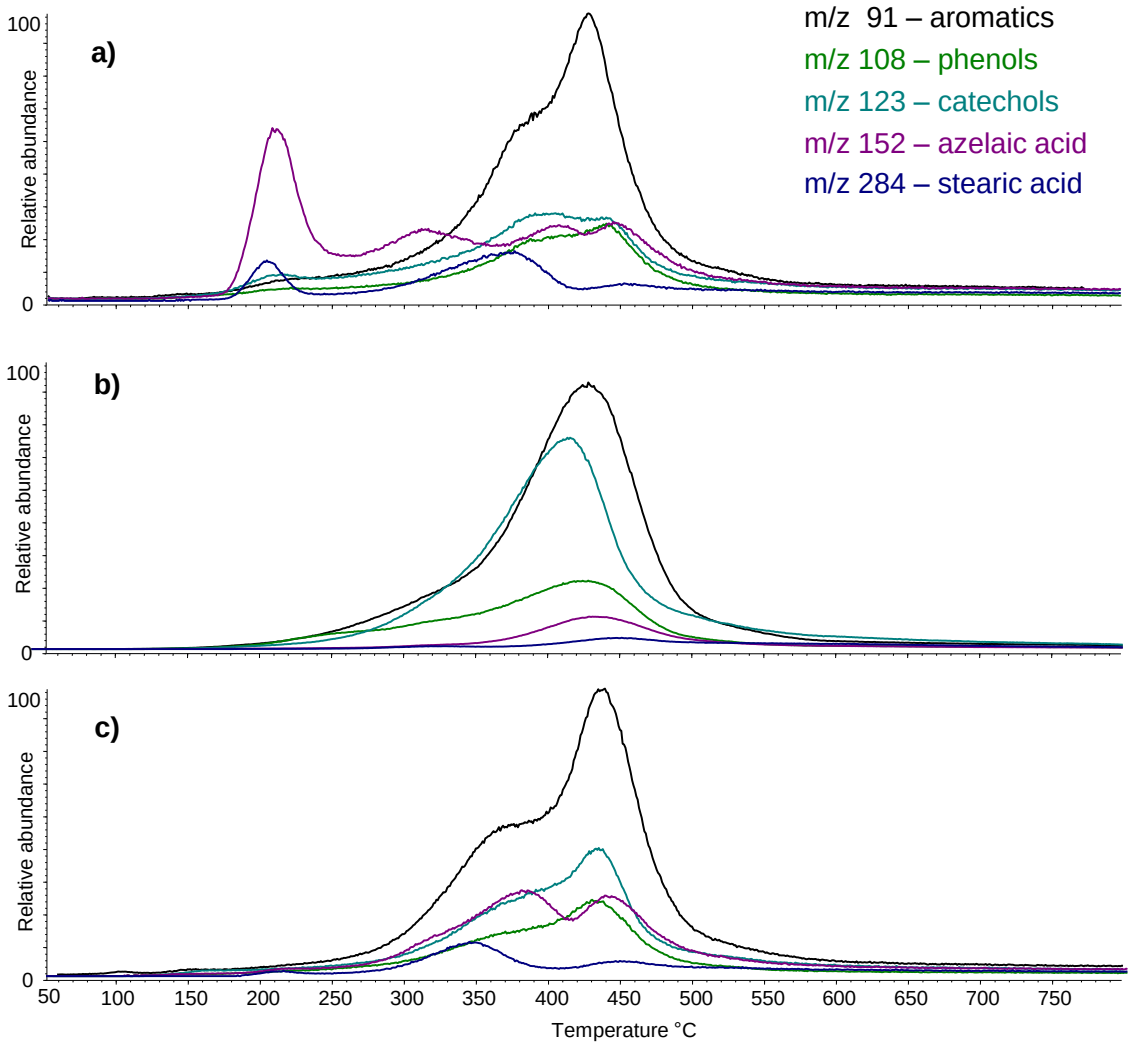

Figure 5. Extract ion thermograms for the fragment ions with *m/z* 91, 108, 123, 152 and 284 obtained by EGA-MS analysis of **a)** tung oil, **b)** urushi and **c)** M1.

The data showed that the free fatty acids present in tung oil were almost absent in the mixtures, suggesting that urushi prevented triglyceride hydrolysis. In addition, the maximum degradation

temperature for aromatics, phenols and catechols was shifted to higher values (from *ca.* 420 to *ca.* 440°C) in the mixture with respect to urushi, highlighting the higher thermal stability of the polymeric network produced in the mixture compared to the pure material.

3.3. HPLC-ESI-Q-ToF. HPLC-ESI-Q-ToF enabled the composition of the triglycerides extracted from the samples to be investigated. Figure 6 shows the extracted ion chromatograms relative to triglycerides obtained for the aged films of tung oil, urushi and the mixture M1.

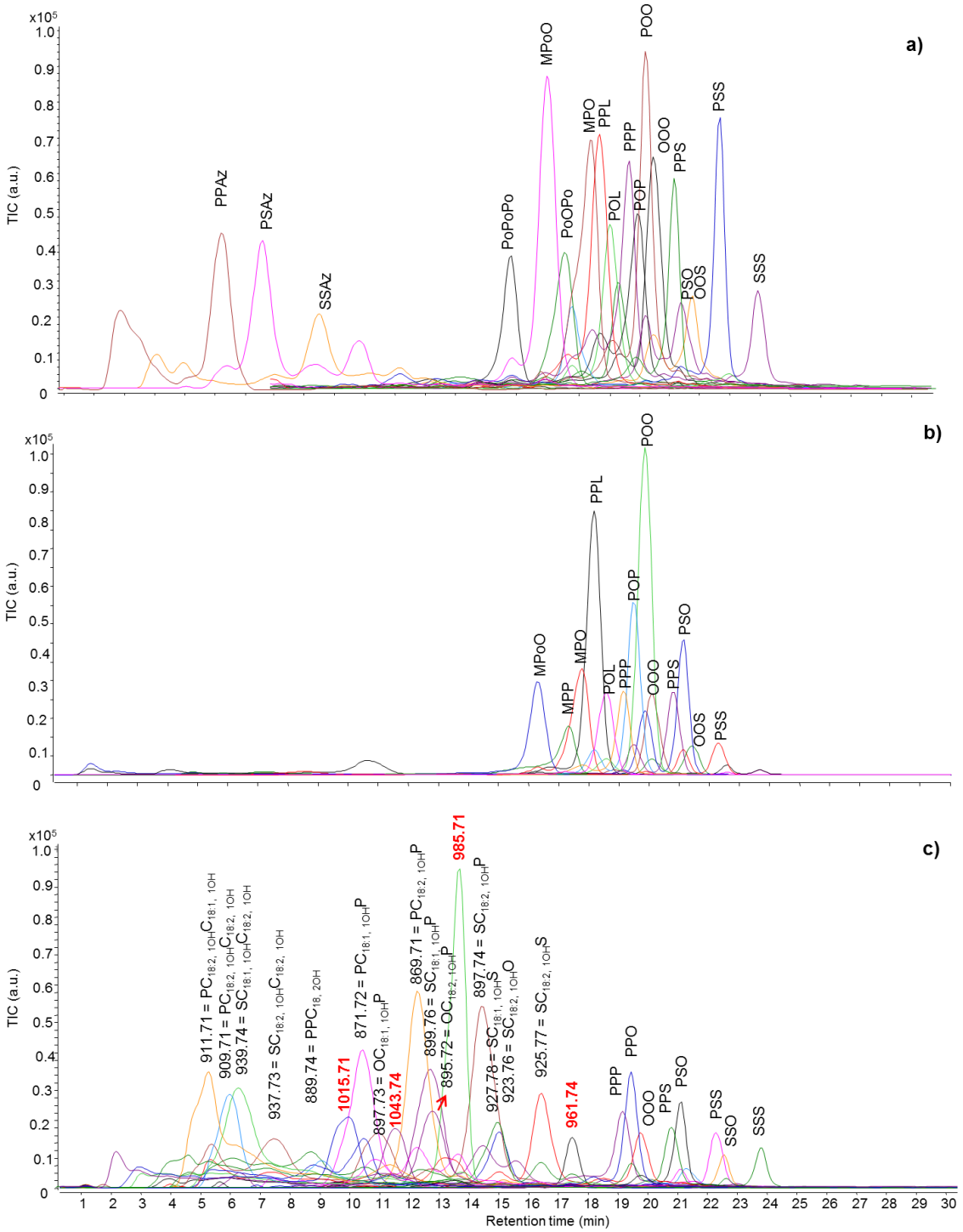

Figure 6. HPLC–ESI-Q-ToF chromatograms of **a)** tung oil, **b)** urushi and **c)** mixture M1. Acyl substituent abbreviations: L, linoleyl (C18:2); O, oleyl (C18:1); S, stearyl (C18:0); Po,

palmitoleyl (C16:1); P, palmityl (C16:0); M, myristyl (C14:0); Az, azelayl (C8COOH). For Cx:y, x represents the number of carbon units and y, the total number of double bonds. Subscript «zOH» refers to the presence of hydroxyl groups, and z represents their number on the acyl substituent.

In tung oil after two years of natural ageing, no triglycerides containing α-eleostearic acid were detected. The most abundant triglycerides were SSS (MH^+ = *m/z* 913.81), OOS (MH^+ = *m/z* 909.79), OOO (MH^+ = *m/z* 907.77), OOL (MH^+ = *m/z* 905.75), PSS (MH^+ = *m/z* 885.79), PSO (MH^+ = *m/z* 883.77), POO (MH^+ = *m/z* 881.75), POL (MH^+ = *m/z* 879.74), PLL (MH^+ = *m/z* 877.73), PPS (MH^+ = *m/z* 857.75), PPO (MH^+ = *m/z* 855.74), PPL (MH^+ = *m/z* 853.72), PPP (MH^+ = *m/z* 829.72), MPO (MH^+ = *m/z* 827.71), MPoO (MH^+ = *m/z* 825.69), PoPoPo (MH^+ = *m/z* 823.67). Some triglycerides containing azelaic acid were also detected, in particular AzSS (MH^+ = *m/z* 817.65), AzSP (MH^+ = *m/z* 789.61) and AzPP (MH^+ = *m/z* 761.59).

Urushi showed the presence of some triglycerides, in agreement with the lipid composition of urushi wax reported in the literature [38]. No oxidised compounds were detected.

The chromatogram of the mixture M1 was dominated by the presence of hydroxylated triglycerides, whereas no triglycerides containing azelaic acid were detected. Hydroxylated fatty acids are intermediate oxidation products of polyunsaturated fatty acids. The data indicated that the tung oil/urushi film presented a relatively lower degree of oxidation with respect to the oil film, as hydroxy acids were still present, and glycerides with dicarboxylic acids were not detectable in the triglyceride fraction.

Ions with *m/z* (961.74, 985.71, 1015. 71 and 1043.74) were also observed in the mass spectra of the mixtures (Figure 6). The tandem MS spectra were similar for all of them, showing, as

main fragmentation pattern, the loss of 308 uma (Figure 7). Although identification of these species was not possible, considering that they are absent in the lipid fraction of tung oil and urushi alone, it is possible that they arise from the molecular interaction taking place between urushi and tung oil.

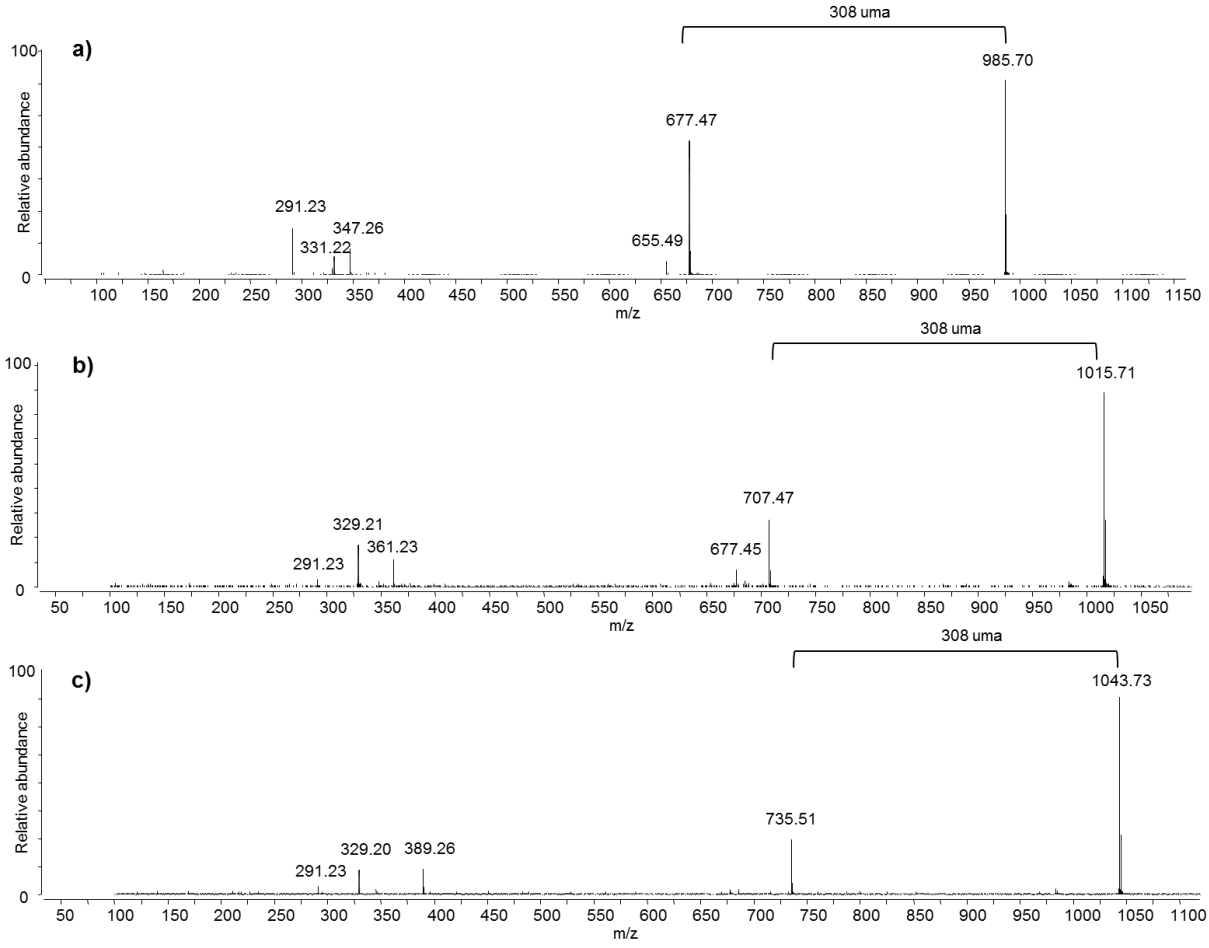

Figure 7. Tandem mass spectra of unidentified ions at *m/z* **a)** 985.70, **b)** 1015.71 and **c)** 1043.73.

3.4. GC-MS. In order to investigate the non-cross-linked fractions of the aged films, GC-MS analysis was performed. The TIC (total ion chromatograms) of tung oil and urushi cured films are reported in Figure 8, and the compounds identified are listed in Table 1.

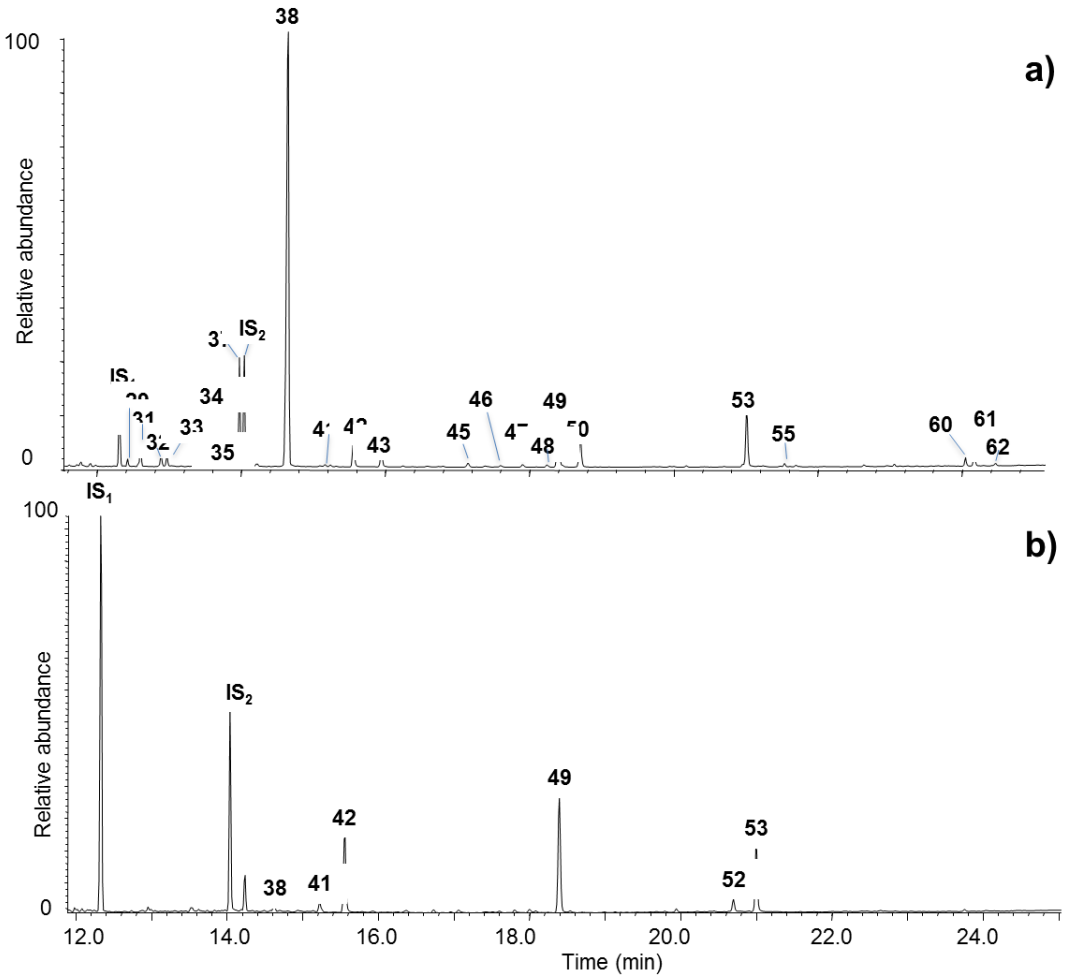

Figure 8. Total ion chromatograms obtained by GC-MS analysis of aged films of **a)** tung oil and **b)** urushi. Peak numbers refer to Table 1.

Table 1. List of compounds identified as trimethylsilyl derivatives in the total ion chromatograms obtained by GC-MS and Py(HMDS)-GC-MS of aged films of tung oil, urushi and their mixtures.

N°	Compound	Principal *m/z*	*GC-MS*	*Py-GC-MS*
IS_1	Hexadecane	57, 71, 85	x	
IS_2	tridecanoic acid	73, 117, 129, 132, 271, 286	x	
1	butanoic acid	75, 117, 145		x
2	propylbenzene [u]	91, 105, 120, 145		x
3	4-pentenoic acid [t]	75, 117, 157		x
4	pentanoic acid	75, 117, 159		x
5	hexenoic acid [t]	75, 117, 129, 171		x
6	hexanoic acid	75, 117, 173		x
7	hydroxyacetic acid [t]	73, 147, 205		x
8	propandioic acid [t]	73, 147, 217		x
9	4-oxo-pentanoic acid [t]	75, 145, 173		x
10	heptenoic acid [t]	75, 117, 129, 185		x
11	heptanoic acid	75, 117, 129, 187		x
12	glycerol (bis-TMS)	73, 103, 117, 131, 147, 218		x
13	1,2,3-trihydroxybutan	59, 73, 117, 131, 147, 205		x
14	1,2-dihydroxybenzene [u]	75, 91, 151, 167, 182		x
15	benzoic acid [u]	51, 77, 105, 135, 179, 194		x
16	octanoic acid	75, 117, 129, 201		x
17	glycerol (tri-TMS)	73, 103, 117, 131, 147, 205, 218		x

18	butandioic acid [t]	73, 129, 147, 247		x
19	2-butendioic acid [t]	73, 117, 129, 147, 245		x
20	nonanoic acid	73, 117, 132, 215		x
21	tetradecene [u]	57, 71, 85, 99, 196		x
22	tetradecane [u]	57, 71, 85, 99, 198		x
23	pentandioic acid	73, 129, 147, 158, 204, 261		x
24	pentadecene [u]	57, 71, 85, 99, 210		x
25	pentadecane [u]	57, 71, 85, 99, 212		x
26	malic acid [t]	73, 147, 233, 245, 335		x
27	hexanedioic acid [t]	73, 129, 147, 172, 275		x
28	decanoic acid [t]	73, 117, 129, 211, 229		x
29	heptandioic acid [t]	73, 129, 147, 173, 289	x	x
30	3-pentylcatechol (mono-TMS) [u]	73, 179, 217, 230, 252		x
31	hydroxyacid [t]	55, 73, 129, 147, 199, 273, 289	x	
32	hydroxyacid [t]	57, 73, 117, 129, 138, 139, 169, 187, 215, 229, 259	x	
33	hydroxyacid [t]	57, 75, 117, 129, 201, 243, 257	x	x
34	octandioic acid (suberic acid) [t]	73, 117, 129, 147, 187, 303	x	x
35	unidentified [t]	57, 73, 103, 117, 129, 147, 213, 287, 303	x	x
36	3-hexylcatechol (mono-TMS) [u]	73, 179, 193, 251, 266		x
37	hydroxyacid [t]	55, 73, 117, 129, 152, 171, 183, 201, 229, 243, 273	x	
38	nonandioic acid (azelaic acid)	73, 117, 129, 147, 201, 317	x	x
39	3-heptylcatechol *(*mono-TMS*)* [u]	73, 179, 265, 280		x

40	hydroxyacid [t]	73, 117, 129, 151, 199, 225, 243		x
41	tetradecanoic acid (myristic acid)	73, 117, 129, 132, 285	x	
42	phthalate (contaminant)	57, 104, 149, 223	x	
43	decandioic acid (sebacic acid) [t]	73, 117, 129, 147, 215, 331	x	x
44	3-octylcatechol *(*mono-TMS*)* [u]	73, 179, 279, 294		x
45	hydroxyacid [t]	73, 95, 129, 147, 213, 303	x	x
46	undecandioc acid [t]	57, 73, 117, 129, 147, 204, 217, 229, 345	x	x
47	hydroxyacid [t]	57, 73, 109, 129, 147, 155, 273, 347	x	
48	hydroxyacid [t]	57, 73, 109, 129, 147, 301, 317	x	
49	hexadecanoic acid (palmitic acid)	73, 117, 129, 145, 313	x	x
50	2-hydroxysebacic acid [t]	55, 73, 109, 129, 147, 301, 317, 391, 419	x	x
51	hydroxyacid [t]	73, 129, 147, 215, 347		x
52	octadecenoic acid (oleic acid)	73, 117, 129, 145, 339, 354	x	x
53	octadecanoic acid (stearic acid)	73, 117, 129, 145, 201, 341, 356	x	x
54	hydroxyacid [t]	73, 117, 129, 147, 229, 303, 361		x
55	benzene derivative [m]	55, 73, 91, 105, 117, 129, 145, 179, 253, 33, 348		x
56	octadecadienoic acid (linoleic acid) [m]	73, 117, 129, 145, 337, 352		x
57	hydroxyacid [t]	57, 73, 129, 147, 204, 217, 245, 365, 445	x	
58	hydroxyacid [t]	73, 117, 129, 147, 218, 243, 317		x

59	hydroxyacid [t]	73, 117, 129, 147, 203, 243, 317, 375		x
60	hydroxyacid [t]	73, 123, 129, 147, 151, 241, 301		x
61	eicosanoic acid [t]	73, 117, 129, 147, 204, 257, 389		x
62	9,10-dihydroxyoctadecanoic acid [t]	55, 73, 129, 147, 215, 317, 390, 518	x	
63	9,10-dihydroxyoctadecanoic acid isomer [t]	55, 73, 129, 147, 215, 317, 390, 518	x	
64	hydroxyacid [t]	57, 73, 129, 147, 207, 215, 317, 341	x	
65	monopalmitin [t]	73, 117, 129, 147, 205, 239, 371		x
66	3-pentadecenylcatechol (mono-TMS) [u]	73, 179, 375, 390		x
67	3-pentadecylcatechol (mono-TMS) [u]	73, 179, 377, 392		x
68	monostearin [t]	73, 117, 129, 147, 205, 399		x

[t] detected only in tung oil; [u] detected only in urushi; [m] detected only in the mixtures; if no letter is indicated, the compound was detected in all samples.

The chromatographic profile of tung oil showed monocarboxylic and dicarboxylic acids as the main compounds, in accordance with the literature [7]. Azelaic acid (#38) was the most abundant compound detected. The formation of dicarboxylic acids as oxidation products of polyunsaturated fatty acids is a significant phenomenon in the autoxidation of drying oils [39]. The detection by GC-MS of azelaic acid with relatively high abundances in cured samples of linseed, walnut and poppyseed oils has been widely reported [5,40,41]. The formation of azelaic acid has been exploited for differentiating drying oils from other lipid sources in historical paintings and works of art [39,42]. In fact, commonly used drying oils in western Europe, such as linseed, walnut

and poppyseed oils, show a ratio between the relative content of azelaic and palmitic acid (A/P ratio) ranging between 1 and 2, and a sum of the relative content of dicarboxylic acids ($\sum D_{\%}$) > 30% [39,41,43]. For linoleic acid ((9*Z*,12*Z*)-9,12-octadecadienoic acid), which is one of the most studied polyunsaturated fatty acids and the most abundant fatty acid in walnut and poppyseed oils, the production of relatively high amounts of azelaic acid can be explained considering that the formation of a radical is favoured in the bis-allylic position (C_{11}) between the two unconjugated double bonds. Radicals and hence hydroperoxides at positions C_9 and C_{13} are thus formed as a consequence of resonance [19]. The decomposition of these hydroperoxides and peroxides coupled to β-scission and further oxidation leads to the formation of azelaic acid [15-17]. Similarities can be found for linolenic acid ((9Z,12Z,15Z)-9,12,15-octadecatrienoic acid), which has two bis-allylic positions and is the most abundant fatty acid in linseed oil.

α-eleostearic acid of tung oil is different because it has three conjugated double bonds. After the abstraction of an H· from the allylic positions (C_8 or C_{15}), the conjugated double bonds create equivalent resonance forms which can theoretically lead, with the same probability, to the formation of hydroperoxides at positions from C_8 to C_{15}. A similar observation has also been reported for the study of conjugated linoleic acid [44]. If the main oxidative pathway of α-eleostearic acid was the same of linoleic and linolenic acids, the main oxidation product of tung oil would be suberic acid (octanedioic acid). However, the results obtained here showed that azelaic acid is the main oxidation product formed from the autoxidation of α-eleostearic acid present in tung oil, and is accompanied by smaller amounts of suberic and sebacic acids. This implies that azelaic acid in tung oil must be formed by the direct addition of oxygen and peroxyl radicals to the double bonds [5,10,13], followed by further oxidation and β-scission reactions, rather than as a consequence of H abstraction, as in the case of linoleic and linolenic acids.

The A/P ratio and $\sum D_{\%}$ obtained in our analyses for tung oil were notably high compared to those generally obtained for other drying oils: 6.4 ± 0.2 and 77% ± 2, respectively. These data seem to indicate that the presence of tung oil in a cured paint film can be hypothesised on the basis of a high A/P ratio.

Palmitic (#49) and stearic (#53) acids were detected, as well as several hydroxy acids (including 2-hydroxysebacic acid (#50) and the two isomers of 9,10-dihydroxyoctadecanoic acid (#60, 61)), which are the intermediate products of oxidation of the original unsaturated fatty acids.

The total ion chromatogram of urushi lacquer showed the presence of myristic (#41), palmitic (#49), oleic (#52) and stearic (#53) acids, confirming the HPLC–ESI-Q-ToF and literature data [38]. Azelaic acid was detected with very low relative abundances (A/P<0.1).

The relative content of azelaic acid observed in the mixtures was significantly lower than the theoretical A/P values estimated on the basis of w/w ratios of urushi/tung oil: A/P= 4 for M1 and A/P= 3 for M4. In particular, the measured A/P ratios were 2.3 ± 0.1, 2.2 ± 0.1 and 1.8 ± 0.1 for M1, M2 and M4, respectively. The data indicated that a lower degree of oxidation of the triglycerides of tung oil is expected when the oil cures in the presence of urushi, in agreement with the results obtained by HPLC–ESI-Q-ToF. The data also indicate that the A/P ratio cannot be used to identify tung oil in a sample of unknown composition, when this also contains urushi in the same layer. These results are in agreement with the literature that the identification of oils in artistic objects containing both a drying oil and the urushi lacquer is very complicated, because the parameters usually used to identify a drying oil are drastically altered [2,45-48], as the A/P ratio is usually reduced compared to those reported for pure drying oils [48].

3.5. Py(HMDS)-GC/MS. Py(HMDS)-GC/MS enabled the polymerised network of the films to be investigated. Figure 9 shows the pyrolytic profiles obtained for aged films of tung oil, urushi and M1. Peak numbers refer to Table 1.

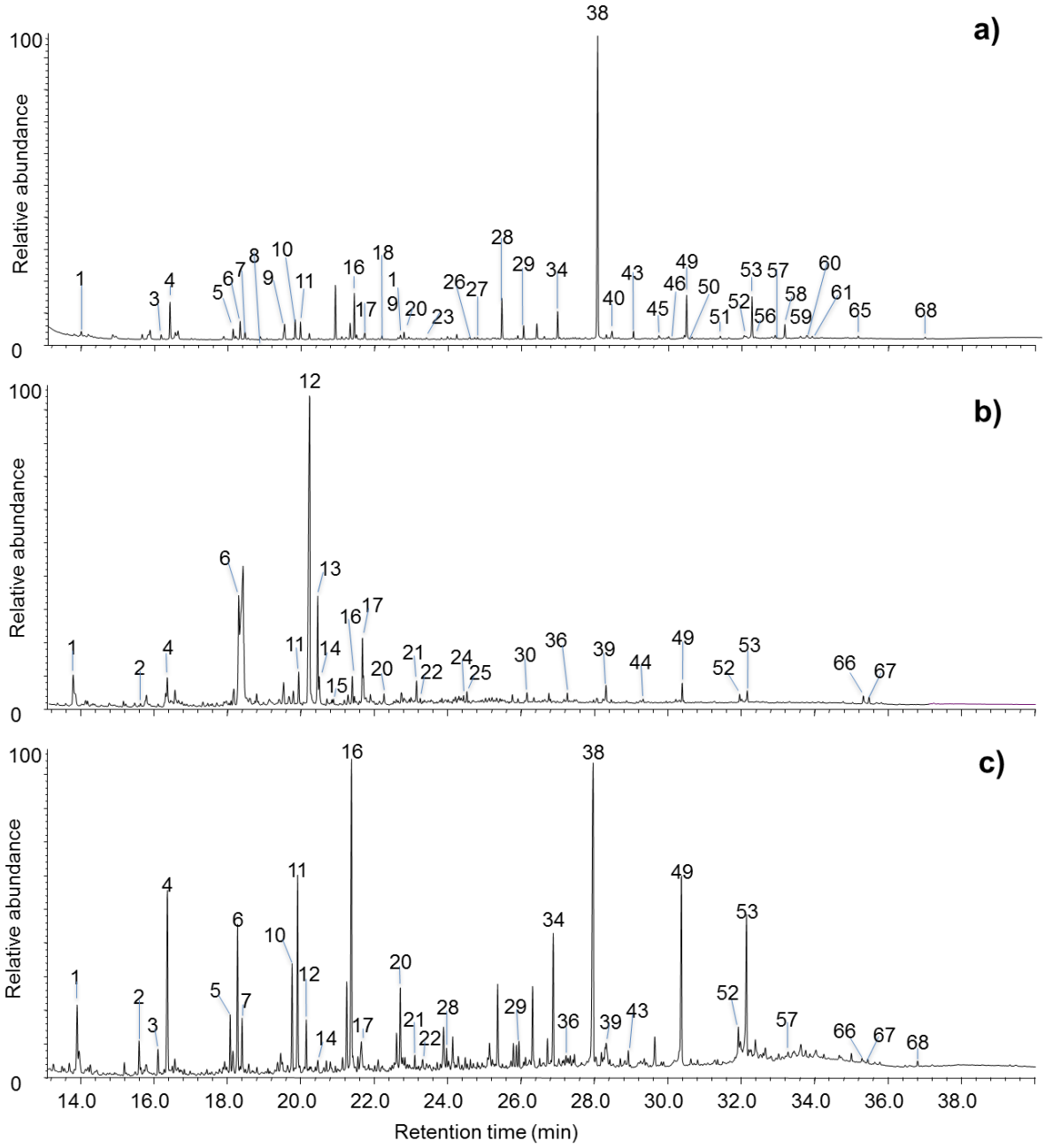

Figure 9. Pyrograms obtained by Py(HMDS)/GC-MS analysis of **a)** tung oil, **b)** urushi and **c)** mixture M1 films. Peak numbers refer to Table 1.

The pyrogram of tung oil is dominated by the peak of azelaic acid, and showed the presence of monocarboxylic, dicarboxylic and hydroxy acids in agreement with the results obtained by GC-MS. Short chain monocarboxylic acids (C5-C9) were also detected with a relatively high abundance, and peaking at C8. The pyrolytic formation of octanoic acid involves a cleavage of the aliphatic side chain between the carbon atoms at positions C_8 and C_9. If the C_9 bears three alkyl substituents, as a consequence of cross-linking reactions, this cleavage is likely to occur, as a secondary radical is produced. Data indicate that C_9 is a favoured position of the cross-linking of α-eleostearic acid.

The pyrogram of urushi showed all the pyrolysis products typical of the lacquer, such as long chain aliphatic hydrocarbons, alkylbenzenes, alkylphenols and alkylcatechols with different degrees of derivatisation [49]. The markers of urushi lacquer 3-pentadecylcatechol (#67) and 3-pentadecenylcatechol (#66) were also detected. Glycerol (#12, 17) was found in the pyrogram of urushi, as also highlighted by EGA-MS analyses.

In the mixtures, in agreement with GC-MS data, a decrease in the relative abundance of azelaic acid was observed. This was accompanied by an increase in the relative abundances of short-chain aliphatic monocarboxylic acids from C5 to C9. A semi-quantitative evaluation[1] was performed in order to estimate the ratio between the relative abundance of octanoic acid and palmitic acid (C8/P ratio). The values obtained were 0.7 ± 0.1 for tung oil and 1.0 ± 0.1, 0.9 ±

[1] Not based on calibration curves but only peak area measurements

0.1, 1.3 ± 0.1 for the mixtures M1, M2 and M4, respectively. The increased production under pyrolysis of short chain fatty acids observed in the mixtures indicates that tung oil polyunsaturated fatty acids are subject to a higher degree of cross-linking when the oil cures in the presence of urushi.

Molecular differences were also visible for urushi. Figure 10 shows the extracted ion chromatograms of the ion with *m/z* 179 for urushi and M1. As previously reported, the extraction of the fragment ion with *m/z* 179 enables the pyrolytic profile of mono-TMS alkylcatechols to be obtained from urushi pyrograms [49].

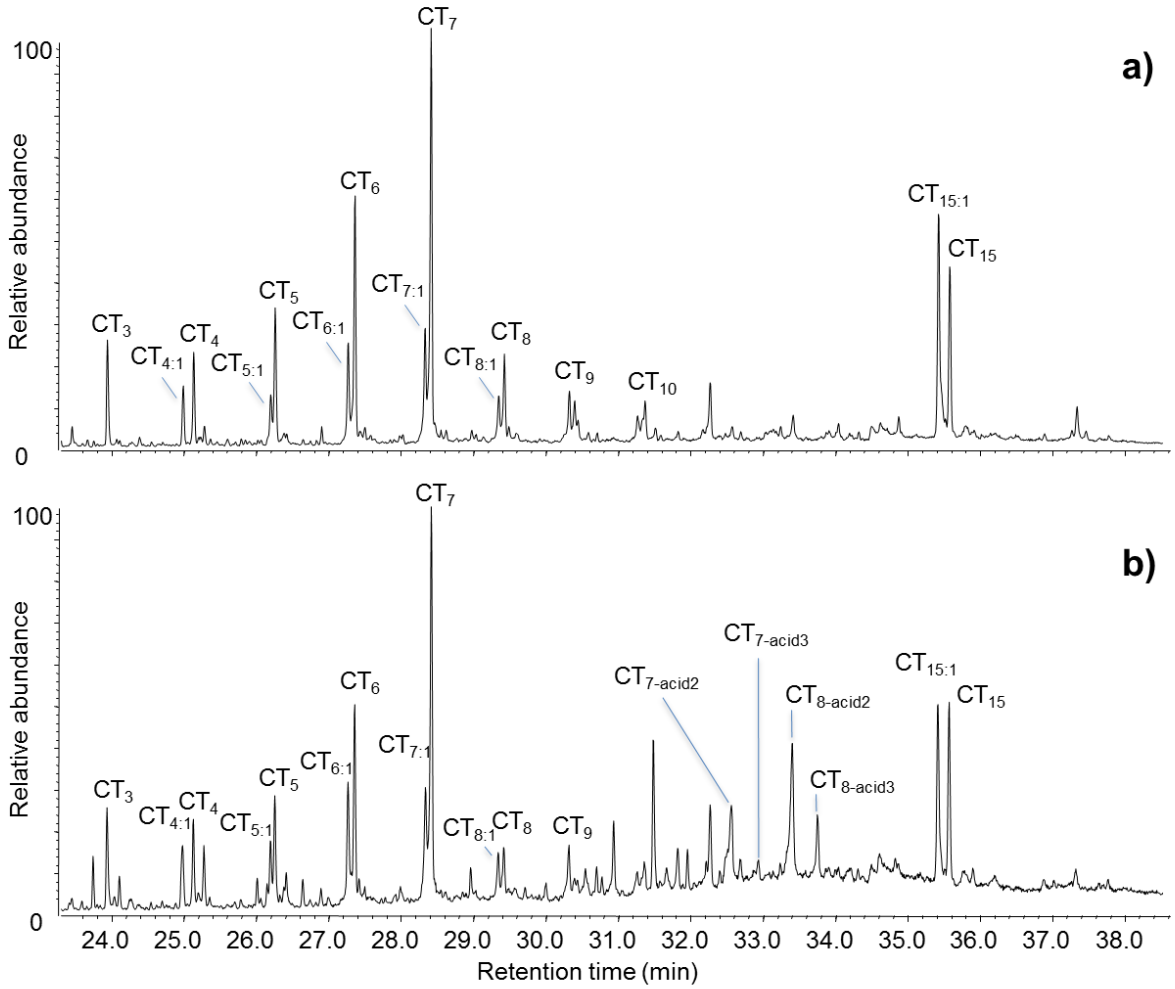

Figure 10. Extracted ion chromatogram of the ion with *m/z* 179: CT3) 3-propylcatechol (TMS); CT4:1) 3-butenylcatechol (TMS); CT4) 3-butylcatechol (TMS); CT5:1) 3-pentenylcatechol (TMS) (#30); CT5) 3-pentylcatechol (TMS); CT6:1) 3-hexenylcatechol (TMS); CT6) 3-hexylcatechol (TMS) (#36); CT7:1) 3-heptenylcatechol (TMS); CT7) 3-heptylcatechol (TMS) (#39); CT8:1) 3-octenylcatechol (TMS); CT8) 3-octylcatechol (TMS) (#44); CT9) 3-nonylcatechol (TMS); CT15:1) 3-pentadecenylcatechol (TMS) (#66); CT15) 3-pentadecylcatechol (TMS) (#67); CT7 $_{acid2}$) 7-(2,3-dihydroxyphenyl)heptanoic acid (2TMS); CT7 $_{acid3}$) 7-(2,3-dihydroxyphenyl)heptanoic acid (3TMS); CT8 $_{acid2}$) 8-(2,3-dihydroxyphenyl)octanoic acid (2TMS); CT8 $_{acid3}$) 8-(2,3-dihydroxyphenyl)octanoic acid (3TMS).

Alkylcatechols with a carboxylic acid functionality at the end of the alkyl chain were detected in the mixtures. In particular, 7-(2,3-dihydroxyphenyl)heptanoic acid and 8-(2,3-dihydroxyphenyl)octanoic acid with different degrees of derivatisation were identified. These compounds have been reported in the literature and are usually ascribed to the oxidation products of the lacquer. However, they have always been identified when the lacquer and a drying oil were both present in the same sample [3,25,49]. Consequently, since the pure lacquer did not show the presence of these compounds, it is reasonable to conclude that the high number of radicals produced by the autoxidation of tung oil favoured the autoxidation of aliphatic substituents of urushi catechols, to an extent that the oxidation products (alkylcatechols with a carboxylic acid functionality at the end of the alkyl chain) became detectable. Since the double bond between C_8 and C_9 is the most abundant in urushi monomers, the oxidation of the allylic position (C_7) and of the first position of the double bond (C_8) is to be expected, thus explaining the presence of 7-

(2,3-dihydroxyphenyl)heptanoic acid and 8-(2,3-dihydroxyphenyl)octanoic acid in the mixtures. It is also worth mentioning that the pyrolytic profiles obtained for the M1 mixture perfectly matched with those obtained for an archaeological sample from our previous publication [49].

4. CONCLUSIONS

A multi-analytical study was performed to investigate the curing mixtures of tung oil and urushi lacquer. The data obtained by both isothermal TG and DSC on these materials, analysed fresh and subsequently at increasing time intervals, indicated that the kinetics and the mechanisms of autoxidation of unsaturated alkyl chains of the tung oil are drastically modified in the presence of urushi, thus suggesting a significant interaction between the two materials during the curing. Oxidation reactions appeared notably reduced in the mixture compared to tung oil, accompanied by an increase in the occurrence of propagation and termination reactions leading to cross-linking.

The application of mass spectrometric techniques on cured films highlighted the molecular aspects of these different curing processes. The composition of the extractable fraction of tung oil was rich in azelaic acid, and the high value of the A/P ratio was notably higher than that found in traditional European drying oils. The tung oil/urushi mixtures showed a drastic reduction in the relative content of azelaic acid and the presence of hydroxylated products, indicating a lower degree of oxidation of the lacquer/oil system with respect to that of pure tung oil. In the mixtures, Py(HMDS)-GC/MS also revealed a relative increase in short-chain aliphatic monocarboxylic acids, which are produced by thermal degradation of the cross-linked network, and EGA-MS highlighted an increased thermal stability of the polymeric network. Cross-linking

and oxidation are competitive reactions that occur during the curing of an oil [10]. All the data indicate that when urushi is added to tung oil, oxidation is slowed down and radicals are more preferably consumed by crosslinking reactions. This can be explained considering that, when mixed with tung oil, urushi acts as an antioxidant, thanks to its high content in catechols. Catechols of urushiol can in fact act as H· donators, stabilising peroxyl radicals formed by autoxidation reactions [50], thus inhibiting reactions following the decomposition of peroxides. The higher content of oxygen incorporated into the network in the mixtures as observed by isothermal TG, must thus be in the form of hydroxyl and ether bonds, rather than acidic moieties.

The formation of oxidised catechol structures was evidence that the unsaturated aliphatic side chains of urushiol are subject to a higher rate of radical autoxidation reactions in the presence of tung oil. This can be explained by hypothesising that the high number of radicals generated by tung oil, and the consequent formation of radicals in the aliphatic side substituents of urushi catechols, lead to the formation of a polymer network containing different structures, which is more thermostable, as observed by EGA-MS.

We believe that this is fundamental in ensuring the formation of a stable, more water repellent film (lower degree of hydrolysis measured by EGA-MS), in which the lipid component of tung oil acts as a plasticiser, which explains the lower levels of hardness of the cured films experimented with by artists.

Finally the data also identified a molecular marker that can be used to determine whether or not the oil was applied in the same layer as urushi. When investigating a painting technique, it is in fact often necessary not only to identify the materials, but also to locate them in the sample stratigraphy [41]. Molecular imaging techniques are not always successful or readily available. This study revealed that, when analysing a sample containing urushi, if a drying oil is identified,

based on a relatively high content of azelaic acid with respect to palmitic acid, the presence in the pyrogram of 7-(2,3-dihydroxyphenyl)heptanoic acid and 8-(2,3-dihydroxyphenyl)octanoic acid tells us that the materials were applied in the same layer, as they cured at the same time.

AUTHOR INFORMATION

Corresponding Author

* E-mail: ilaria.bonaduce@unipi.it

Notes

The authors declare no competing financial interest

Present Addresses

† Present address: Department of Scientific Research, The British Museum, Great Russell Street, London WC1B 3DG.

Author Contributions

The manuscript was written through contributions of all authors. All authors have given approval to the final version of the manuscript.

ACKNOWLEDGMENTS

The authors wish to thank Prof. Erwin Emmerling (Technische Universität, Munich, Germany), who bought the raw material in China; Dr. Catharina Blaensdorf (Technische Universität, Munich, Germany), who provided the sample, and Dr. Luca Bernazzani (University of Pisa) for the useful discussions on DSC data.

REFERENCES

(1) Mazzeo, R.; Cam, D.; Chiavari, G.; Fabbri, D.; Ling, H.; Prati, S.: Analytical study of traditional decorative materials and techniques used in Ming Dinasty wooden architecture. The case of the Drum Tower in Xi'an, P.R of China. *Journal of Cultural Heritage* **2004**, *5*, 273-283.

(2) Ling, H.; Maiqian, N.; Chiavari, G.; Mazzeo, R.: Analytical characterization of binding medium used in ancient Chinese artworks by pyrolysis–gas chromatography/mass spectrometry. *Microchemical Journal* **2007**, *85*, 347-353.

(3) Heginbotham, A.; Schilling, M.: New Evidence for the use of Southeast Asian raw materials in seventeenth-century Japanese export lacquer. In *East Asian Lacquer: Material Culture, Science and Conservation*; Rivers, S., Faulkner, R., Boris Pretzel, R., Eds.; Archetype Publications: London, 2011; pp 92-106.

(4) Yang, X.; Zhang, S.; Li, W.: The performance of biodegradable tung oil coatings. *Progress in Organic Coatings* **2015**, *85*, 216-220.

(5) Mills, J. S.; White, R.: *The Organic Chemistry of Museum Objects*, 1994.

(6) Zhang, L.; Jia, B.; Tan, X.; Thammina, C. S.; Long, H.; Liu, M.; Wen, S.; Song, X.; Cao, H.: Fatty Acid Profile and Unigene-Derived Simple Sequence Repeat Markers in Tung Tree (Vernicia fordii). *PLoS ONE* **2014**, *9*, e105298.

(7) Schonemann, A.; Frenzel, W.: An investigation of the fatty acid composition of new and aged tung oil. *Studies in conservation* **2006**, *51*, 99-110.

(8) Soucek, M. D.; Khattab, T.; Wu, J.: Review of autoxidation and driers. *Progress in Organic Coatings* **2012**, *73*, 435-454.

(9) Porter, N. A.; Weber, B. A.; Weenen, H.; Khan, J. A.: Autoxidation of polyunsaturated lipids. Factors controlling the stereochemistry of product hydroperoxides. *Journal of the American Chemical Society* **1980**, *102*, 5597-5601.

(10) Oyman, Z. O.; Ming, W.; van der Linde, R.: Oxidation of drying oils containing non-conjugated and conjugated double bonds catalyzed by a cobalt catalyst. *Progress in Organic Coatings* **2005**, *54*, 198-204.

(11) Muizebelt, W. J.; Hubert, J. C.; Nielen, M. W. F.; Klaasen, R. P.; Zabel, K. H.: Crosslink mechanisms of high-solids alkyd resins in the presence of reactive diluents. *Progress in Organic Coatings* **2000**, *40*, 121-130.

(12) Muizebelt, W. J.; Donkerbroek, J. J.; Nielen, M. W. F.; Hussem, J. B.; Biemond, M. E. F.; Klaasen, R. P.; Zabel, K. H.: Oxidative crosslinking of alkyd resins studied with mass spectrometry and NMR using model compounds. *Journal of Coatings Technology* **1998**, *70*, 83-93.

(13) Brimberg, U. I.; Kamal-Eldin, A.: On the kinetics of the autoxidation of fats: substrates with conjugated double bonds. *European Journal of Lipid Science and Technology* **2003**, *105*, 17-22.

(14) Muizebelt, W. J.; Nielen, M. W. F.: Oxidative Crosslinking of Unsaturated Fatty Acids Studied with Mass Spectrometry. *Journal of Mass Spectrometry* **1996**, *31*, 545-554.

(15) Mallégol, J.; Gardette, J.-L.; Lemaire, J.: Long-term behavior of oil-based varnishes and paints. Photo- and thermooxidation of cured linseed oil. *Journal of the American Oil Chemists' Society* **2000**, *77*, 257-263.

(16) Mallégol, J.; Gardette, J.-L.; Lemaire, J.: Long-term behavior of oil-based varnishes and paints. Fate of hydroperoxides in drying oils. *Journal of the American Oil Chemists' Society* **2000**, *77*, 249-255.

(17) Chan, H. W.-S.; Prescott, F. A. A.; Swoboda, P. A. T.: Thermal decomposition of individual positional isomers of methyl linoleate hydroperoxide: Evidence of carbon-oxygen bond scission. *Journal of the American Oil Chemists' Society* **1976**, *53*, 572-576.

(18) Duce, C.; Della Porta, V.; Tiné, M. R.; Spepi, A.; Ghezzi, L.; Colombini, M. P.; Bramanti, E.: FTIR study of ageing of fast drying oil colour (FDOC) alkyd paint replicas. *Spectrochimica Acta Part A: Molecular and Biomolecular Spectroscopy* **2014**, *130*, 214-221.

(19) Passi, S.; Picardo, M.; De Luca, C.; Nazzaro-Porro, M.; Rossi, L.; Rotilio, G.: Saturated dicarboxylic acids as products of unsaturated fatty acid oxidation. *Biochimica et Biophysica Acta (BBA) - Lipids and Lipid Metabolism* **1993**, *1168*, 190-198.

(20) Lu, R.; Yoshida, T.; Miyakoshi, T.: Oriental Lacquer: A Natural Polymer. *Polymer Reviews* **2013**, *53*, 153-191.

(21) Niimura, N.; Miyakoshi, T.; Onodera, J.; Higuchi, T.: Identification of ancient lacquer film using two stage pyrolysis-gas chromatography/mass spectrometry. *Archeometry* **1999**, *41*, 137-149.

(22) Oshima, R.; Yamauchi, Y.; Watanabe, C.; Kumanotani, J.: Enzymic oxidative coupling of urushiol in sap of the lac tree, Rhus vernicifera. *The Journal of Organic Chemistry* **1985**, *50*, 2613-2621.

(23) Xia, J.; Lin, J.; Xu, Y.; Chen, Q.: On the UV-Induced Polymeric Behavior of Chinese Lacquer. *Applied Materials and Interfaces* **2011**, *3*, 482–489.

(24) Watanabe, H.; Fujimoto, A.; Nishida, J.; Ohishi, T.; Takahara, A.: Biobased Polymer Coating Using Catechol Derivative Urushiol. *Langmuir* **2016**, *32*, 4619-4623.

(25) Wei, S.; Song, G.; He, Y.: The identification of binding agent used in late Shang Dynasty turquoise-inlayed bronze objects excavated in Anyang. *Journal of Archaeological Science* **2015**, *59*, 211-218.

(26) Taguchi, K.; Hirose, S.; Abe, Y.: Photo-curing composite paint containing urushi (Oriental lacquer), and wrinkled coating caused by phase separation. *Progress in Organic Coatings* **2007**, *58*, 290-295.

(27) Harigaya, S.; Honda, T.; Rong, L.; Miyakoshi, T.; Chen, C.-L.: Enzymatic dehydrogenative polymerization of urushiols in fresh exudates from the lacquer tree, Rhus vernicifera DC. *Journal of agricultural and food chemistry* **2007**, *55*, 2201-2208.

(28) Watanabe, H.; Fujimoto, A.; Takahara, A.: Spray-Assisted Nanocoating of the Biobased Material Urushiol. *Langmuir* **2015**, *31*, 2360-2365.

(29) La Nasa, J.; Zanaboni, M.; Uldanck, D.; Degano, I.; Modugno, F.; Kutzke, H.; Tveit, E. S.; Topalova-Casadiego, B.; Colombini, M. P.: Novel application of liquid chromatography/mass spectrometry for the characterization of drying oils in art: Elucidation on the composition of original paint materials used by Edvard Munch (1863–1944). *Analytica Chimica Acta* **2015**, *896*, 177-189.

(30) Lluveras-Tenorio, A.; Mazurek, J.; Restivo, A.; Colombini, M. P.; Bonaduce, I.: The development of a new analytical model for the identification of saccharide binders in paint samples. *PLOS ONE* **2012**, *7*, e49383.

(31) Lazzari, M.; Chiantore, O.: Drying and oxidative degradation of linseed oil. *Polymer Degradation and Stability* **1999**, *65*, 303-313.

(32) Litwinienko, G.; Jodko-Piórecka, K.: Recent Developments in DSC Analysis to Evaluate Thermooxidation and Efficacy of Antioxidants in Vegetable Oils. In *Differential Scanning Calorimetry*; CRC Press, 2014; pp 49-74.

(33) Guiotto, E. N.; Ixtaina, V. Y.; Nolasco, S. M.; Tomás, M. C.: Effect of Storage Conditions and Antioxidants on the Oxidative Stability of Sunflower–Chia Oil Blends. *Journal of the American Oil Chemists' Society* **2014**, *91*, 767-776.

(34) Duce, C.; Bernazzani, L.; Bramanti, E.; Spepi, A.; Colombini, M. P.; Tiné, M. R.: Alkyd artists' paints: do pigments affect the stability of the resin? A TG and DSC study on fast-drying oil colours. *Polymer Degradation and Stability* **2014**, *105*, 48-58.

(35) Ploeger, R.; Scalarone, D.; Chiantore, O.: Thermal analytical study of the oxidative stability of artists' alkyd paints. *Polymer Degradation and Stability* **2009**, *94*, 2036-2041.

(36) Mallégol, J.; Gonon, L.; Commereuc, S.; Verney, V.: Thermal (DSC) and chemical (iodometric titration) methods for peroxides measurements in order to monitor drying extent of alkyd resins. *Progress in Organic Coatings* **2001**, *41*, 171-176.

(37) Ouldmetidji, Y.; Gonon, L.; Commereuc, S.; Verney, V.: A differential scanning calorimetry method to study polymer photoperoxidation. *Polymer Testing* **2001**, *20*, 765-768.

(38) Jin, Z.-L.; Tada, A.; Sugimoto, N.; Sato, K.; Masuda, A.; Yamagata, K.; Yamazaki, T.; Tanamoto, K.: Analysis of Constituents in Urushi Wax, a Natural Food Additive. *Food Hygiene and Safety Science (Shokuhin Eiseigaku Zasshi)* **2006**, *47*, 167-172.

(39) Colombini, M. P.; Modugno, F.; Ribechini, E.: GC/MS in the characterization of lipids. In *Organic Mass Spectrometry in Art and Archeology*; Colombini, M. P., Modugno, F., Eds.; Wiley: Chichester (UK), 2009; pp 191-213.

(40) Bonaduce, I.; Ribechini, E.; Modugno, F.; Colombini, M. P.: Analytical Approaches Based on Gas Chromatography Mass Spectrometry (GC/MS) to Study Organic Materials in Artworks and Archaeological Objects. *Topics in Current Chemistry* **2016**, *374*, 1-37.

(41) Bonaduce, I.; Carlyle, L.; Colombini, M. P.; Duce, C.; Ferrari, C.; Ribechini, E.; Selleri, P.; Tiné, M. R.: New Insights into the Ageing of Linseed Oil Paint Binder: A Qualitative and Quantitative Analytical Study. *PLoS ONE* **2012**, *7*, e49333.

(42) Colombini, M. P.; Andreotti, A.; Bonaduce, I.; Modugno, F.; Ribechini, E.: Analytical Strategies for Characterizing Organic Paint Media Using Gas Chromatography/Mass Spectrometry. *Accounts of Chemical Research* **2010**, *43*, 715-727.

(43) van den Berg, J. D. J.; van den Berg, K. J.; Boon, J. J.: Identification of non-cross-linked compounds in methanolic extracts of cured and aged linseed oil-based paint films using gas chromatography–mass spectrometry. *Journal of Chromatography A* **2002**, *950*, 195-211.

(44) Hämäläinen, T. I.; Sundberg, S.; Mäkinen, M.; Kaltia, S.; Hase, T.; Hopia, A.: Hydroperoxide formation during autoxidation of conjugated linoleic acid methyl ester. *European Journal of Lipid Science and Technology* **2001**, *103*, 588-593.

(45) Wei, S.; Pintus, V.; Pitthard, V.; Schreiner, M.; Guoding Song, G.: Analytical characterization of lacquer objects excavated from a Chu tomb in China. *Journal of Archaeological Science* **2011**, *38*, 2667-2674.

(46) Heginbotham, A.; Khanjian, H.; Rivenc, R.; Schilling, M.: A procedure for the efficient and simultaneous analysis of Asian and European lacquers in furniture of mixed origin. In *15th Triennial Conference, New Delhi, 22-26 September 2008: Preprints (ICOM Committee for Conservation)*; Bridgland, J., Ed.; Allied Publishers: New Delhi, 2008; pp 608-616.

(47) Liu, X.; Cristina, T.; Maria, V.: A Preliminary Study of Three Finishing Materials for Traditional Chinese Furniture. *Advances in Materials Physics and Chemistry* **2014**, *4*, 85-92.

(48) Pitthard, V.; Wei, S.; Miklin-Kniefacz, S.; Stanek, S.; Griesser, M.; Schreiner, M.: Scientific investigations of antique lacquers fron a 17th-century japanese ornamental cabinet. *Archaeometry* **2010**, *52*, 1044–1056.

(49) Tamburini, D.; Bonaduce, I.; Colombini, M. P.: Characterization and identification of urushi using in situ pyrolysis/silylation–gas chromatography–mass spectrometry. *Journal of Analytical and Applied Pyrolysis* **2015**, *111*, 33-40.

(50) Foti, M. C.: Antioxidant properties of phenols. *Journal of Pharmacy and Pharmacology* **2007**, *59*, 1673-1685.